

Three Phases in the Evolution of Leonid Meteor Trains

By

Jiří BOROVIČKA* and Pavel KOTEN*

(1 February 2003)

Abstract: We present image intensified video observations of spectra of persistent meteor trains during Leonids 2001. Three distinct phases of the train evolution were found. The first two phases show atomic line spectra but both spectra are different by the presence of lines of higher excitation in the second phase. We interpret the first phase, which lasts only few seconds, as a rapid cooling of gas under non-equilibrium conditions. The second phase, lasting tens of second, was found to be driven by atomic recombinations. The third phase shows continuous spectrum which emerges about 20 seconds after the train formation and persists for minutes. Several molecular species are probably responsible for the luminosity but they could not be reliably identified.

1. OBSERVATIONS

We report here observations of persistent meteor trains performed with image intensified video cameras during the 2001 Leonid meteor shower. The observations were done at two sites in Arizona, USA, the Mt. Lemmon Observatory (110°788 W, 32°442 N, 2791 m) and the Crystal Forest station (109°890 W, 34°793 N, 1667 m). Slitless spectroscopy with 600 grooves/mm objective gratings and second generation Dedal 41 image intensifiers was performed. A 1.4/50 mm lens providing field of view of 25° and spectral resolution 11.5 Å/mm was used most of the time. A 2/85 mm lens with 15° field of view and 7 Å/mm was used part of the time.

Both cameras were used for continuous recording and taking meteor spectra. When a fireball appeared and persistent train was formed somewhere on the sky, the camera was moved and, if necessary, the grating rotated to get the train spectrum. In total, nine first order train spectra were obtained this way. The time interval between the train formation and the capture of its spectrum ranged between 4 and 90 seconds. In one case, the spectrum of the mother fireball was taken in high spectral orders. That record also contained 0.8 s of the initial stage of the train evolution. The train spectrum was then observed in the first order at the second station starting 18 s after the formation.

This paper is based on the analysis of two well observed trains. The first is the above mentioned train observed at both stations. The mother fireball occurred on November 17 at

* Astronomical Institute, Academy of Sciences, 251 65 Ondřejov Observatory, The Czech Republic

12:57:23 UT during the morning twilight, one day before the Leonid peak. We refer to this train as to Train 1. The second analyzed train, Train 6, was formed on November 18 at 11:01:02 UT during the first Leonid peak. It was observed with the 85 mm lens from 5 s after the formation.

When watching the records, one can easily distinguish three phases of the evolution of the train spectra. At the beginning, the train intensity decreases rapidly and the spectrum is dominated by atomic line emissions. We call this phase *the afterglow*. The afterglow of another Leonid fireball was studied in detail by Borovička & Jenniskens (2000, hereafter referred to as Paper I). The second phase is also dominated by atomic lines but the spectrum is different and the intensity of the lines decreases slowly. We call this phase, which persists for about 40 seconds, *the line phase*. After about 20 s after train formation a continuous emission emerges and persists for minutes. We call this *the continuum phase*. In the following, we will analyze the spectra of the three phases separately.

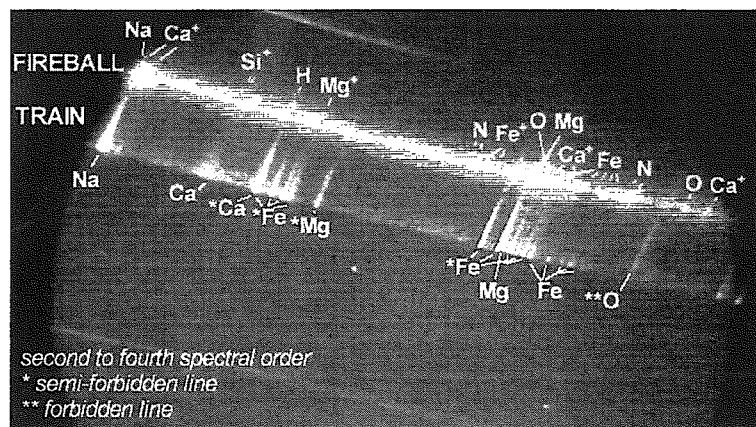


Fig. 1: A superposition of two video frames showing the spectrum of the fireball just before maximum brightness and the spectrum of the train just after the fireball disappearance. The wavelengths increase from the left to the right and the spectrum starts with the overlapping lines of Na (5893 Å) in the second order and Ca⁺ (3933 Å) in the third order.

2. THE AFTERGLOW

In Fig. 1 the spectra of the fireball and the afterglow are compared. They are quite different. In accordance with previous findings, the fireball spectrum contains also lines of high excitation and/or ionization of both meteoric (Ca⁺, Mg⁺, Si⁺, Fe⁺, H) and atmospheric origin (N, O). These lines are absent in the afterglow spectrum. On contrary, the afterglow spectrum contains low excitation intercombination (semi-forbidden) lines of Fe, Mg, and Ca with low transition probability. Also the forbidden green oxygen line is present. The only lines common to both spectra are low and medium excitation lines with high transition probability of Na, Fe, Ca, and Mg. See Paper I for a detailed line identification.

The line decay rate was found to be proportional to the upper excitation potential, i.e. the intensity decrease is slowest for the lines with lowest excitation potential. After a fraction of second, the spectrum is dominated by lines with excitation potential less than 3 eV, regardless of transition probability. This behavior was explained in Paper I by a rapid cooling of gas under non-equilibrium conditions. Low electron density in the train causes non-Boltzmann population of levels in atoms. In general, the intensity of a line, I , is proportional to the number of atoms in the upper state, N_i , and the transition probability A_{ij} :

$$I \sim h\nu N_i A_{ij}, \quad (1)$$

where h is the Planck constant and ν is the frequency of the transition. Here we assume that the train is optically thin. Since $h\nu$ and A_{ij} are atomic constants, the actual line intensities depend on the level populations. Since the atomic processes are extremely short in comparison with the lifetime of the train, the level population can be estimated from the condition of statistical equilibrium. Under the conditions in the afterglow, atomic levels are depopulated mainly by radiative and collisional deexcitation and populated by collisional excitation from the ground level. The frequencies of these processes are proportional to:

$$\text{radiative deexcitation} \sim N_i A_i \quad (2)$$

$$\text{collisional deexcitation} \sim N_i C_{i0} = N_i n_e Q_i \quad (3)$$

$$\text{collisional excitation} \sim N_0 C_{0i} = N_0 n_e Q_i e^{-E_i/kT}. \quad (4)$$

Here $A_i = \sum_{j < i} A_{ij}$ is the radiative deexcitation rate, C is the collisional transition probability, n_e is free electron density, Q_i is a function slightly dependent on temperature, E_i is the excitation potential, k is Boltzmann constant and T is temperature. Combining the above equations, we find that the level population is proportional to

$$N_i \sim \frac{N_0 e^{-E_i/kT}}{A_i/n_e Q_i + 1}. \quad (5)$$

To explain the afterglow spectrum, we found a typical value of $n_e Q_i \approx 10^5 \text{ s}^{-1}$. The allowed transitions ($A_i \approx 10^8 \text{ s}^{-1}$) are weakened relatively to the semi-forbidden transitions ($A_i \approx 10^3 \text{ s}^{-1}$) in comparison with thermal equilibrium conditions when $A_i \ll n_e Q_i$ for all lines. We ignored the statistical weight of levels in this order-of-magnitude computation.

3. THE LINE PHASE

The spectra of both trains in the line phase are shown in Fig. 2. Detailed line identification is given in Table 1. The spectrum is different from the spectrum of afterglow by the presence of lines of relatively high excitation. The magnesium line at 5180 Å with excitation potential of 5.1 eV is one of the brightest lines.¹ Lines up to excitation potential 7 eV are present. The lines of high excitation persist in the spectrum and do not decay more quickly than the low excitation lines. The intensities of three lines as a function of time are shown in Fig. 3. There might be even intensity increase in some lines after the rapid decay of the afterglow, in the time period which, unfortunately, was not well covered by observations.

¹ In fact, this Mg line is blended with a low excitation Fe line. However, the Fe line contributes only a minor part of the intensity as can be seen on the Fe line at 5110 Å which has always nearly the same intensity as the Fe line at 5170 Å. The Fe and Mg lines are separated in the third order spectrum of the afterglow. The Mg line is much fainter there than the Fe lines (see Fig. 1).

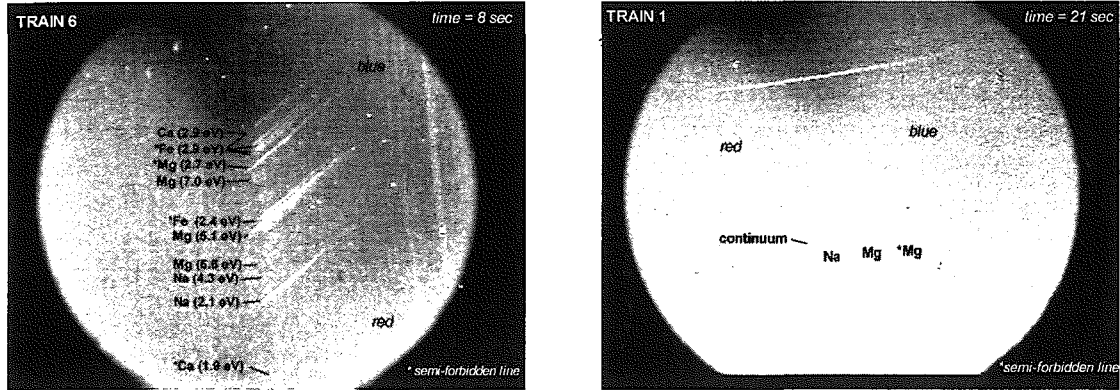


Fig. 2: The spectrum of Train 6 at 8 sec after formation (left) and Train 1 at 21 sec after formation (right). The images were obtained by averaging dozens of video frames to reduce the noise of the image intensifier. Spectral lines are identified.

Table 1: Line identification for Train 6 at time 8 sec. The observed wavelength [\AA] and intensity in arbitrary units (but corrected for spectral sensitivity of the camera) is given for each line. The identification is given in form of laboratory wavelength, atom, and multiplet number. The excitation potential [eV] and radiative deexcitation rate [s^{-1}] of the upper level is also given as well as the radiative transition probability for the line [s^{-1}]. 2.2+4 means 2.2×10^4 .

λ_{obs}	I	λ_{lab}		E_i	A_i	A_{ij}	λ_{obs}	I	λ_{lab}		E_i	A_i	A_{ij}
4210	22	4216	Fe I 3	2.94	2.2+4	1.8+4	5173		Mg I 2	5.11	1.0+8	3.5+7	
		4207	Fe I 3	3.00	1.1+4	7.1+3	5169		Fe I 1	2.45	4.2+3	3.6+3	
		4227	Ca I 2	2.93	2.2+8	2.2+8	5166		Fe I 1	2.40	1.4+3	1.4+3	
4375	16	4376	Fe I 2	2.83	3.0+4	3.0+4	5260	4.5	5270	Fe I 37	3.96	4.2+6	3.7+6
4425	11	4427	Fe I 2	2.85	4.6+4	4.5+4	5400	0.9	5435	Fe I 15	3.29	1.1+7	1.7+6
		4435	Fe I 2	2.88	1.7+4	4.7+3			5406	Fe I 15	3.28	1.2+7	1.1+6
4460	8.5	4462	Fe I 2	2.87	3.0+4	3.0+4			5371	Fe I 15	3.27	1.2+7	1.0+6
		4482	Fe I 2	2.88	2.3+4	2.1+4	5530	1.3	5528	Mg I 9	6.59	2.0+7	2.0+7
		4490	Fe I 2	2.88	1.7+4	1.2+4	5690	1.0	5688	Na I 6	4.28	1.9+7	1.2+7
4570	9	4571	Mg I 1	2.71	4.3+2	4.3+2			5683	Na I 6	4.28	1.9+7	1.0+7
4700	1.5	4703	Mg I 11	6.98	2.6+7	2.6+7	5895	8	5890	Na I 1	2.10	6.2+7	6.2+7
4755	1.2	4752	Na I 11	4.71	2.8+6	1.3+6			5896	Na I 1	2.10	6.2+7	6.2+7
		4748	Na I 11	4.71	2.8+6	6.3+5	6170	1	6161	Na I 5	4.12	7.8+6	5.2+6
4985	0.6	4983	Na I 9	4.59	7.5+6	4.9+6			6162	Ca I 3	3.91	8.6+7	4.8+7
		4979	Na I 9	4.59	7.5+6	4.1+6			6166	Ca I 20	4.53	2.2+7	2.2+7
5110	4.5	5110	Fe I 1	2.42	5.1+3	4.9+3	6360	1	6359	Fe I 13	2.81	4.3+2	4.3+2
5180	14	5184	Mg I 2	5.11	1.0+8	5.7+7	6570	1	6573	Ca I 1	1.89	2.6+3	2.6+3

The spectrum of Train 1 varied with height at this phase. This was well visible on color photographs taken from Mt Lemmon by J. Kac (private communication²). The upper part of the train is blue while the lower part is yellow. The spectrum (Fig. 2) shows that the Mg lines extend higher than the Na line. The blue color was likely supported also by the Mg multiplet 3 at 3830 \AA , where the image intensifier is not sensitive.

The physical mechanism behind the line radiation must be different than that in the afterglow phase because the spectrum and its time evolution is different. We need a physical

² see <http://www.orion-drustvo.si/MBKTeam/meteors/leo2001photoaz.htm>

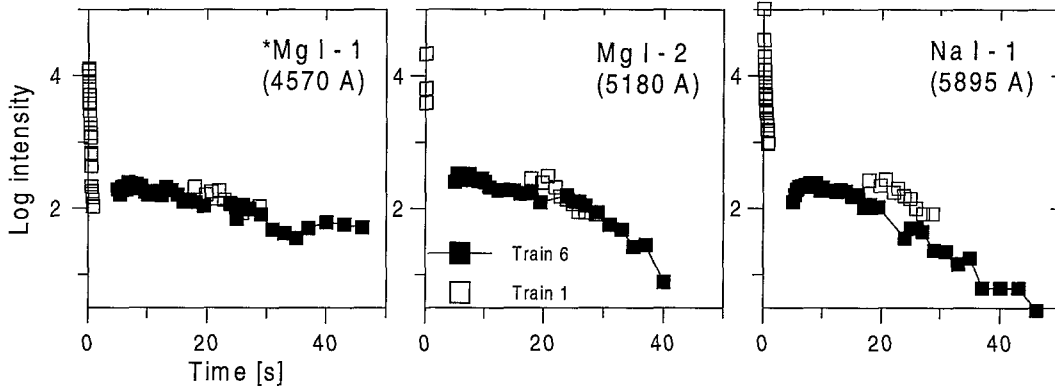


Fig. 3: Intensities of three lines in two trains as a function of time. Intensities are in arbitrary units.

mechanism to excite atomic levels up to at least 7 eV. Thermal collisions are insufficient because train temperature was much lower than 1000 K at this time. Chemical reactions are hardly so exothermal to provide enough energy. We therefore propose that atomic recombination followed by electron downward cascade is responsible for the population of high levels. This process was previously discarded as the explanation of meteor train luminosity (Cook & Hawkins 1956), nevertheless that conclusion was not based on train spectra and must be revised.

The population of a level due to recombination is proportional to:

$$\text{recombination} \sim n_e N^+ \alpha(T, E_i) \approx n_e N^+ \alpha_0(T) e^{-E_i/D}, \quad (6)$$

where N^+ is the number of single ionized atoms and α is the recombination coefficient for a given level. Here the recombination coefficient includes also recombinations to higher levels which then contribute to the population of the given level by downward cascading. It would be very difficult to compute this coefficient for each level. We therefore assumed the dependence on excitation potential to be of a simple exponential form and introduced the constant D . This is rather a fitting formula than a physically justified approach but it can explain the observed spectrum surprisingly well as we will see below. We can neglect collisional excitation in the line phase because of low temperature. The statistical equilibrium can be therefore computed from Eqs. (2), (3) and (6). The resulting formula for level population is

$$N_i \sim \frac{n_e N^+ \alpha_0(T) e^{-E_i/D}}{A_i + n_e Q_i}. \quad (7)$$

Using this formula and Eq. (1), the observed spectrum was fitted. A good fit was obtained by putting $n_e Q_i = 10^4 \text{ s}^{-1}$ and $D = 0.84 \text{ eV}$ for all elements. The values of $N^+ \alpha_0$ must be, naturally, different for each element. The spectrum was fitted only on relative scale, so the relative values of $N^+ \alpha_0$ for five elements to the value for iron were adjusted and are given in Table 2. The comparison of the observed and computed spectrum is given in Fig. 4. A Gauss profile was assigned to the computed lines to simulate the resolution of the observed spectrum. The agreement is very good, all lines could be explained and only in few cases there is a significant discrepancy in the intensity (eg. the lines at 4755 and 5260 Å). Considering all simplification we made, the number of discrepancies is surprisingly small. We therefore consider recombination to be a likely mechanism to produce the line phase of the train. The

only not well understood aspect is the high abundance of Mg ions relatively to Fe ions (see Table 2), because both the ionization potential and recombination coefficient of Mg and Fe are similar (Shull & Steenberg 1982).

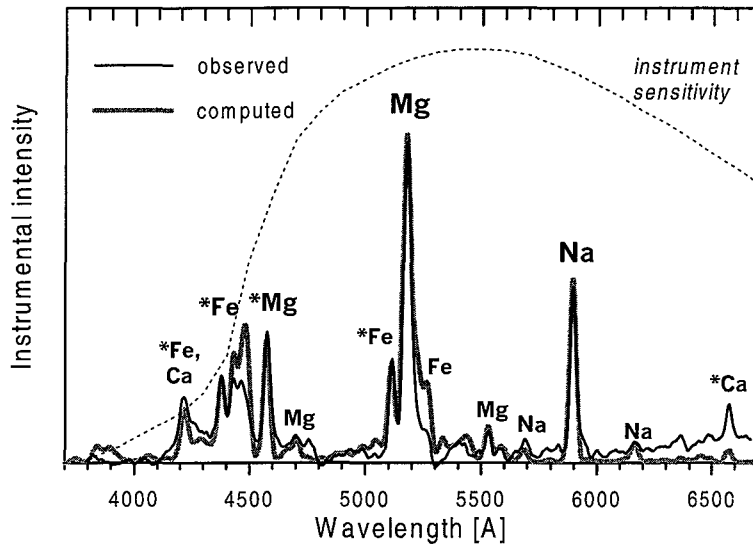


Fig. 4: The comparison of the observed and computed spectrum of Train 6 at 8 seconds. The computed spectrum was multiplied by the spectral sensitivity curve of the instrument, which is also given.

Table 2: The product of the number of ions and the recombination coefficient relative to iron needed to fit the spectrum of Train 6 at 8 sec. Relative chondritic abundances of atoms are given for comparison.

Element	$(N^+ \alpha_0)_{El} / (N^+ \alpha_0)_{Fe}$	Chondritic abundance relative to Fe
Mg	20	1.2
Na	0.3	0.06
Ca	0.2	0.07
Cr	0.05	0.015
Mn	< 0.02	0.01

Nice spectra of Leonid trains in the line phase were presented at this conference by Suzuki (2002). He covered a spectral range mostly different from us (3750–4500 and 7500–9500 Å) and detected a number of other emissions of Na I, Mg I, Al I, Si I, and Fe I. All can be explained by the recombination mechanism. He also detected molecular bands of O₂ and OH, where other mechanisms may be involved.

For a definitive confirmation of the recombination mechanism, a quantitative analysis must be done in the future. A preliminary order-of-magnitude estimate suggests that recombination is plausible to explain the train luminosity. The total luminosity of bright lines such as the Mg lines at 4570 and 5180 Å over the bright part of Train 6 (about 1.5 km long) corresponded to about 10²⁰ emitted photons per second. The product $n_e N^+ \alpha_0$ for Mg should therefore be $\sim 10^{23} \text{ s}^{-1}$. Since $\alpha_0 \approx 10^{-12} \text{ cm}^3 \text{ s}^{-1}$, that number can be achieved with the luminous volume of the order of 10¹² cm³ (length 1.5 km, radius ~ 15 m), $n_e \sim 10^{12} \text{ cm}^{-3}$, and $N^+ \sim 10^{23}$ (i.e.

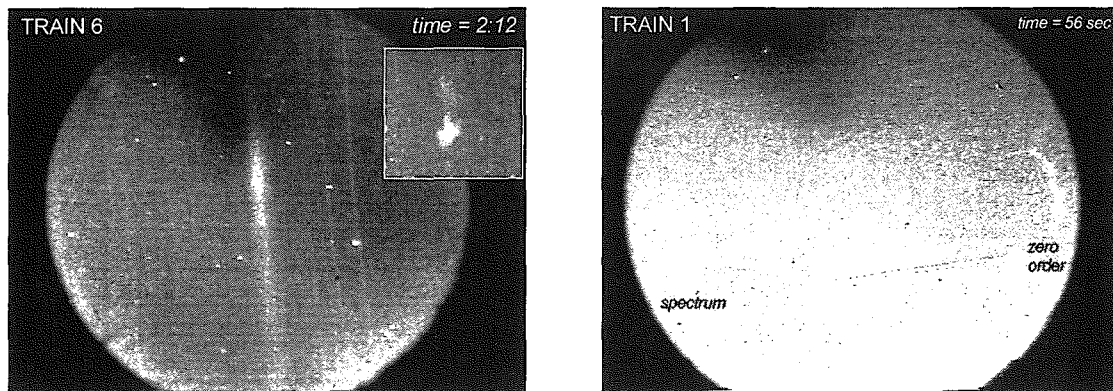


Fig. 5: The spectrum of Train 6 at 2 minutes 12 sec after the formation with the direct image of the train (zero order) taken shortly afterwards in the inset (left). A part of the spectrum of Train 1 at 56 sec after formation together with the image of the train (right). The images were obtained by averaging dozens of video frames to reduce the noise of the image intensifier.

the density of ions of 10^{11} cm^{-3}). The total number of 10^{23} Mg ions corresponds to few grams of Mg. Since more than half of Mg atoms is expected to be ionized during the meteor phase (at $T \sim 5000 \text{ K}$) and Mg may represent about 10% of meteoroid mass, an initial meteoroid mass of the order of tens of grams is needed – a value quite possible for a Leonid fireball. The assumed electron density is, however, rather high. Such number of electrons can be produced during the fireball passage, but such a high electron density does not correspond to the low value of $n_e Q_i$. The solution could be a ion-ion recombination, which could also account for the absence of the Na line at higher altitudes (Baggaley 1977).

4. THE CONTINUUM PHASE

At the time 20–30 s after the train formation, when the atomic lines weakened, a featureless continuum appeared in the yellow and red part of the spectrum. The intensity of the continuum increased at the beginning, then became stable and later decreased gradually as the train dispersed. The continuum phase is evidently responsible for the persistence of meteor trains for minutes or longer. While the train at the line phase still approximately follows the meteor path, we found that the continuum may become strong at only some points along the train and the train then becomes deformed soon.

The images of train spectra in the continuum phase are shown in Fig. 5. The continuum was probably caused by some molecular emissions excited by chemical reactions. No clear band structure which would help to identify the source is, however, evident. Several identification were proposed in the past on the basis of train observations: FeO (Jenniskens et al. 2000), NO₂ (Paper I), OH (Clemesha et al. 2001). Theoretical work considered the emissions of FeO and other metal oxides, NO₂, SO₂, Fe, Na, O₂ (Baggaley 1976, Murad 2001, Kruschwitz et al. 2001). In Fig. 6 we compare the observed spectrum with the laboratory spectrum of FeO. There is some similarity in the position of the maxima, nevertheless the FeO bands are not well pronounced in the observed spectrum. There is also additional luminosity in the red and infrared part of the spectrum with possible maximum at $\sim 7500 \text{ \AA}$ but the low sensitivity of the instrument in this region prevents to say more. FeO probably contributes to the spectrum but cannot explain all

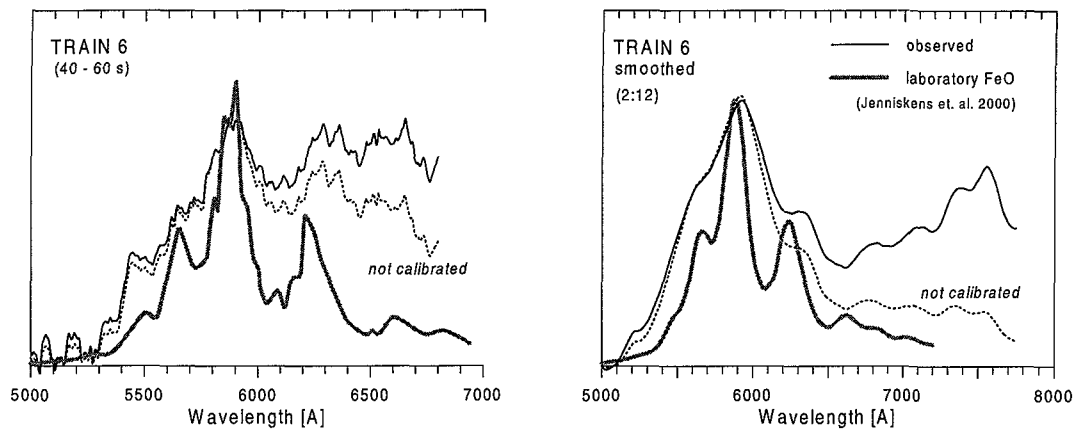


Fig. 6: The observed spectra of Train 6 at two times compared with the laboratory spectrum of FeO (taken from Jenniskens et al. 2000). The dashed line represent the observed signal without calibration to spectral sensitivity of the instrument.

luminosity. Possible other contributors can be OH, NO₂ and CaO. The presence of OH bands in other phases of train evolution (Suzuki 2002, Abe et al. 2002) supports that identification. Nevertheless, definite answer on the nature of persistent continuous emission in meteor trains can be obtained only by using high resolution slit spectroscopy.

5. CONCLUSIONS

We have identified three distinct phases in the evolution of persistent Leonid trains. The first phase is an afterglow, lasting just few seconds. The spectrum is dominated by atomic lines of low excitation. Physically, this phase can be explained by rapid cooling of gas under non-equilibrium conditions. The second phase lasts for tens of seconds and is characterized by atomic lines of low and medium excitation. The source of the luminosity seems to be atomic recombination. Finally, the last phase which can last for minutes is characterized by a continuous spectrum. We can speculate that chemiluminescence is responsible for this phase but the exact species involved are to be identified. The three phases described in this paper are typical for Leonid trains, though individual trains can differ in details as indicated by a preliminary survey of other data.

ACKNOWLEDGMENTS

We thank Javor Kac for providing color pictures of the trains. This work was supported by grant no. 205/02/0982 from GAČR and the presentation was supported by the International Symposium Grant of the Japanese Ministry of Education, Culture, Sports, Science and Technology (MEXT) and the Institute of Space and Astronautical Science (ISAS), Japan. The observation at Mt. Lemmon was a part of the ground support for the 2001 Leonid MAC.

REFERENCES

- Abe S., Yano H., Ebizuka N. et al., 2002, this conference.
 Baggaley W.J., 1976, Mon. Not. R. astr. Soc. 174, 617.

- Baggaley W.J., 1977, *Bull. Astron. Inst. Czech.* 28, 108.
- Borovička J., Jenniskens P., 2000, *Earth, Moon and Planets* 82-83, 399 (Paper I).
- Clemesha B.R., de Medeiros A.F., Gobbi D. et al., 2001, *Geophys. Res. Let.* 28, 2779.
- Cook A.F., Hawkins G.S., 1956, *Astrophys. J.* 124, 605.
- Jenniskens P., Lacey M., Allan B.J., Self D.E., Plane J.M.C., 2000, *Earth, Moon and Planets* 82-83, 429.
- Kruschwitz C.A., Kelley M.C., Gardner C.S. et al., 2001, *J. Geophys. Res.* 106, 21525.
- Murad E., 2001, *Meteoritics Planet. Sci.* 36, 1217 .
- Shull J.M., Steenberg M.V., 1982, *Astrophys. J. Suppl. Ser.* 48, 95.
- Suzuki S., 2002, this conference.